お茶の水女子大学自然科学報告　第71巻　特別号
Natural Science Report, Ochanomizu University, Vol. 71, Special Issue（2020）

Transcranial Cortex-Wide Fluorescence Imaging through a Fully Intact Skull, as a Powerful Tool for Functional Mapping: Less Invasive Macroscopic Imaging of Cortical Ca^{2+} Dynamics

Hiromu Monai*[,1,2]

[1]Department of Biology, Faculty of Science, Ochanomizu University,2-1-1 Ohtsuka, Bunkyo-ku, Tokyo 112-8610, Japan, [2]Center for Brain Science, RIKEN, 2-1 Hirosawa, Wako-shi, Saitama 351-0198, Japan

* monai.hiromu@ocha.ac.jp

(Received May 15, 2020)

Abstract

Astrocytes are neural cells that play an essential role in the modulation of neurotransmission and synaptic plasticity in the brain, yet the main target of neurophysiological research has been neural networks. One reason is that astrocytes show less fluctuation in their membrane potentials, unlike neurons, and it is difficult to evaluate their activity by electrical measurements. On the other hand, the Ca^{2+} imaging technique has revealed that astrocytes can vary widely in intracellular Ca^{2+} concentration. In our laboratory, we use a transgenic mouse line (G7NG817) that expresses G-CaMP7, a Ca^{2+} sensor protein, in astrocytes and a portion of the excitatory neurons, to visualize cortical function *in vivo*. As G7NG817 mice show a dense expression of G-CaMP7 in the cerebral cortex, it is possible to image brain Ca^{2+} dynamics without thinning the skull using standard epifluorescence microscopy. The advantage of this transcranial cortex-wide imaging technique is to observe the more native and stable activity of a wide field of view even under awake conditions compared to the conventional open-skull imaging method because it induces less stress and inflammation in the brain. Using the G7NG817 mouse, we have reported that specific neuronal populations in the cortex were activated by distinct modalities, such as light, sound, or whisker mechanical stimulation. It is confirmed that regional and rapid responses were due to neuronal activities. On the contrary, astrocytes showed more global and slower dynamics than neurons. We found that it is possible to discriminate neuronal and astrocytic activities, even under transcranial imaging, by the different dynamics of the Ca^{2+} event. In this review, we will review the recent development of the fully intact transcranial cortex-wide Ca^{2+} imaging technique, and in the latter part, introduce some practical examples of G7NG817 mice.

1. Introduction

The brain is a black box; the function of the brain is not able to be known just by observations from the outside. However, the brain's electromagnetic activities can be visualized and measured using the electroencephalogram (EEG) and magnetoencephalogram (MEG). Blood flow and metabolic flow change can be detected using functional magnetic resonance imaging (fMRI) and positron emission tomography (PET).

One of the brain cells, neurons, conducts electric information measuring a membrane potential using an electrode and can electrically detect the activity of the cells. Electrophysiological measurements can provide a precise temporal resolution but poor spatial resolution. To understand the causal relationship between single neurons in the neural network, monitoring cellular activities with a higher spatial resolution is necessary.

Fluorescence imaging is a technique to visualize neural activities such as the change in membrane potentials

and intracellular calcium ion (Ca^{2+}) concentrations in a field of view simultaneously by a fluorescence-tagged sensor. Another advantage of this technique is that it is less invasive than electrophysiology, using photons instead of penetrating electrodes. It is known that the neuron increases intracellular Ca^{2+} with its electrical activities.

Furthermore, it is difficult to evaluate the activities of astrocytes, a type of non-neuronal brain cell, by electrophysiological means because it is much less responsive to electrical impulses compared to neurons. Therefore, people have believed that astrocytes are just supporting neurons, and their contribution to active brain functions like information processing has been overlooked for a long time. However, it has been reported that astrocytes also show dynamic intracellular Ca^{2+} elevation when imaged by Ca^{2+} fluorescence, which we refer to as Ca^{2+} imaging.

Ca^{2+} imaging with a chemical indicator was invasive due to the use of a loading electrode to inject the dye into the brain tissue, and most dye quickly induces phototoxicity of the drug. Recently, the development of various types of transgenic animals that express Ca^{2+}-sensitive fluorescent proteins enables us to observe brain activities in living animals, in a less invasive, less toxic, and continuous manner.

Since the brain tissue is highly scattering, Visible wavelengths are unable to penetrate to the deeper areas of the brain. The thinnest part of the cerebral cortex of mice is at least 800–900 μm; however, standard epifluorescence microscopy can only observe at most a few hundred μm from the surface of the brain with a single photon illumination. Whereas, two-photon microscopy employing a specialized scanning laser enables us to observe the deeper area, more than 800 μm from the surface. Besides, as the focal plane is quite limited (not contaminated with other focal planes), observations with two-photon microscopy is very suitable for the analysis of not only the structure of the neural networks, but also the spatiotemporal relationship between neurons and astrocytes.

The visualization and tracking of the information flow at multiple and extensive fields are essential because nerve cells make a vast network as a whole in the brain. Indeed, fMRI and PET are some of the prevalent non-invasive macroscopic functional imaging tools, which can visualize a metabolic change following neural activities with some contrast agents to enhance the signals. Still, they need professional and expensive facilities. Meanwhile, the recent field of view of two-photon microscopy, which is conventionally at most 500–600 μm, is substantially larger at a few mm, which is large enough to visualize over 10,000 cells simultaneously [1–3]. However, to monitor cellular activities, so far, it has been needed to remove the cranial bone with the method known as the open-skull method or craniotomy, which could damage brain tissue.

The open-skull method is a highly technical surgery to remove only the skull (usually less than 0.2 mm)—sometimes dura as well—and implant a coverslip. It takes quite a long time to learn the technique. Additionally, it is highly possible that an electric drill to open the skull damages the tissue and induces severe bleeding. Alternatively, without open craniotomy, the thinning skull has been attracting attention, but it is still technically challenging.

Instead, recent transgenic technologies enable us to monitor the brain activities through the skull, i.e., transcranial imaging with relatively lower spatial resolution, but a larger field of view to the extent possible to functional imaging. Multiple kinds of literature have reported that transcranial imaging is practical for monitoring the wide-field information flow across the broad brain regions [4–25]. Notably, this technique is useful for the initial evaluation of the cortical function in disease models [13].

This review will introduce the fully intact transcranial macroscopic imaging, cortex-wide Ca^{2+} imaging, as practical applications.

2. A brief history of the cortex-wide transcranial Ca^{2+} imaging

Classically, transcranial imaging in living animals has been used to visualize the auto-fluorescence changes corresponding to local metabolic changes, for example, intrinsic optical imaging [26–28] and flavin-based fluorescent protein imaging [29,30]. Large craniotomy

enabled hemisphere-wide imaging with membrane voltage-sensitive dyes [31,32] and Ca^{2+} sensors [33,34]. In the case of imaging without craniotomy, the thinning skull of transgenic mice also enables cortex-wide imaging [35–38].

In 2014, Vanni and Murphy reported the first case of fully intact transcranial imaging with transgenic mice that express genetically encoded Ca^{2+} indicator (GECI), that is, GCaMP3 [4]. They sealed the surface of the cranial bone with dental cement to keep transparency and put a large cover glass to monitor chronically [4,7]. Afterward, the transcranial imaging has been established to observe the cortex-wide functional connectivities across the broad brain region [4–25]. Using transcranial cortex-wide imaging, the group of Timothy Murphy at the University of British Columbia has demonstrated a way to calculate functional connectivity in murine cerebral cortex in both healthy and pathological brain. Moreover, they have consistently reported that the distinct functional connectivity between the sensory cortex and motor cortex seems to exhibit a regular spatiotemporal pattern [4,6,7,18]. Besides, the group of Fritjof Helmchen at the University of Zurich reported that using the paradigm of the whisker-based texture discrimination task, distinct signal flow pathways could sustain the short term-memory or refine sensory learning in mice. Furthermore, the disturbance of this separate route could impair the performance of mice [15,25]. Therefore, transcranial cortex-wide imaging will be a powerful tool to reveal new features of brain dynamics.

3. Transcranial cortex-wide Ca^{2+} imaging with G7NG817 transgenic mice

For transcranial imaging, multiple transgenic mice which express various GECIs have been developed; for example, mainly GCaMP3 [4,10], GCaMP6f [6,9,15,17–19,25], GCaMP6s [6,7,11,12,14,20–23], and YC2.60 [16], and also some unique genetically encoded proteins like extracellular glutamate sensor iGluSnFR [8,12]. We generated a transgenic mouse line that expresses G-CaMP7 (the hyphen is officially needed), that is, G7NG817 mice [39], as shown in Figure 1. We have demonstrated the usefulness of G7NG817 mice in the fully intact transcranial imaging [5,13,24,40].

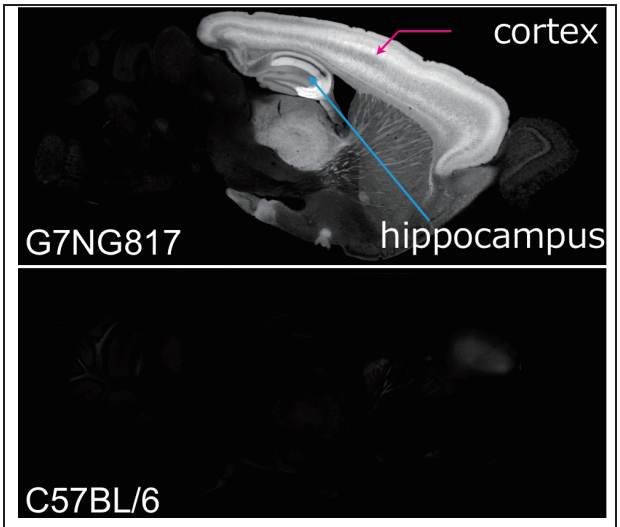

Fig. 1. Fluorescent expression pattern of the sagittal section of fixed mouse brains. (top) G7NG817 line transgenic mouse, (bottom) C57BL/6 line wild-type mouse as a control (Modified from Monai et al., 2016 [5])

The G7NG817 mouse expresses G-CaMP7 under the control of the glutamate transporter-1 (GLT-1) promotor, aiming to monitor the activity of cerebral astrocytes [5]. GLT-1 has been known to be dominantly expressed on the astrocytic membrane to uptake glutamate. We confirmed G-CaMP7 expression in almost 100% of astrocytes and a subpopulation of excitatory neurons in the cortex, in which the expression pattern correctly reflects previously reported results [41], that is, higher expression in layers 4 and 6, and then layer 2/3 (Fig. 1). We also confirmed that GABAergic interneuron and another kind of glia, such as IBA-1 positive microglia did not express G-CaMP7. Interestingly, the cerebral cortex so densely expresses G-CaMP7 that it enables us to observe the cortical activities through the skull by using standard epifluorescence microscopy.

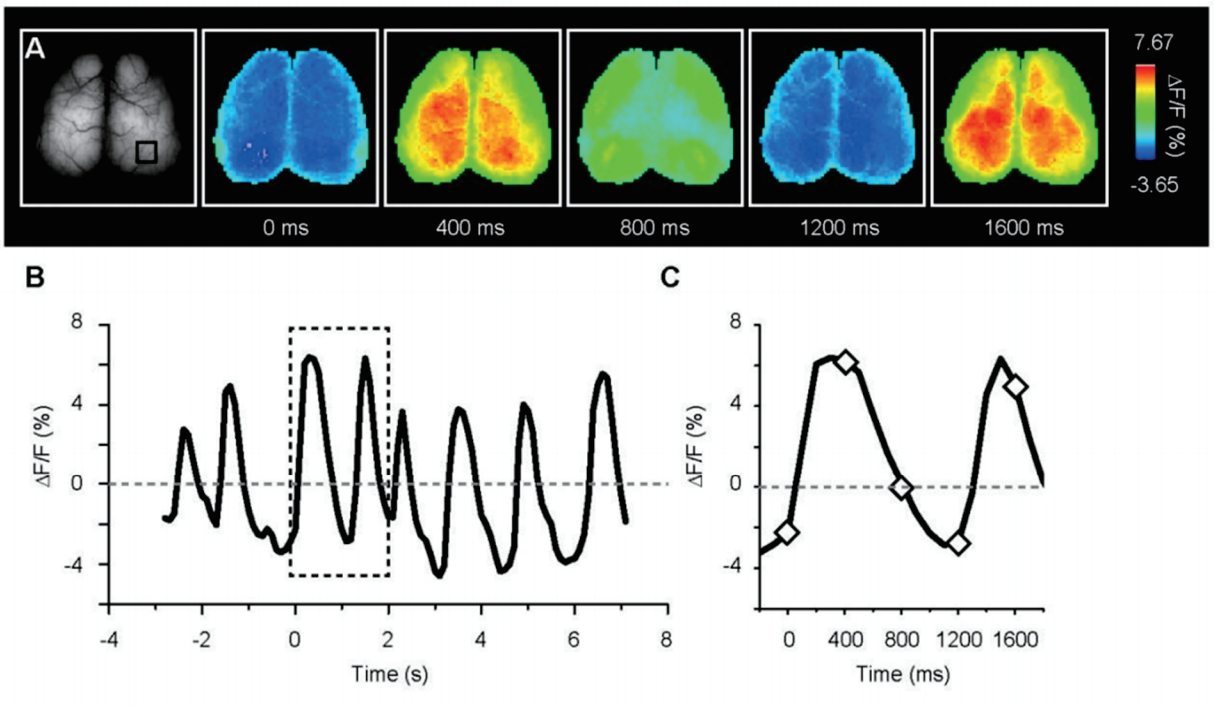

Fig. 2. Spontaneous Ca^{2+} oscillation in deeply anesthetized G7NG817 mouse. (A) Representative images of Ca^{2+} oscillations. Pseudocolor is superimposed on the raw brain images. (B) Example trace of fluorescence change ratio in the black square drawn in A. The baseline is the mean of all-time course. The sampling rate is 10 Hz. (C) Magnified trace in the dotted line in B. The diamonds correspond to the time point shown in A (Modified from Monai et al., 2016 [5]).

The skull of a mouse is thin and transparent enough to see the brain surface through it but only immediately after opening the scalp. Removing the connective tissue on the scalp induces it to promptly dry out and lose transparency. Therefore, if we stop the evaporation of the water from the skull, it is possible to maintain transparency for a long time. For this purpose, people have proposed to drop silicone oil onto the skull for an acute experiment, and transparent dental cement for continuous observation.

In our experiments, mice were anesthetized with urethane (1.6 g/kg), and the body temperature was maintained at 37 °C with a heating pad during surgery and recording. The mouth and nose were tightly fixed to stereotaxic using an auxiliary ear bar to remove the effect of pulsation and respiration. We applied a mixture of liquid paraffin and Vaseline (1:1) immediately after the removal of connective tissue on the skull surface.

Figure 2 shows a spontaneous Ca^{2+} oscillation of urethane-anesthetized G7NG817 mice. The frequency of the up-down state was 0.5–0.2 Hz, which corresponds to the electroencephalogram known as a delta wave. Corresponding areas between the left and right hemispheres almost synchronized. Interestingly, active and inactive regions seemed to alternately emerge (See Monei et al. [5], Supplementary Movie 1, https://www.nature.com/articles/ncomms11100#Sec24). Comparing to the cortical map, which is drawn by using voltage-sensitive dye imaging [32], even spontaneous activities under deep anesthesia, in different sensory regions such as visual or auditory, were found at random.

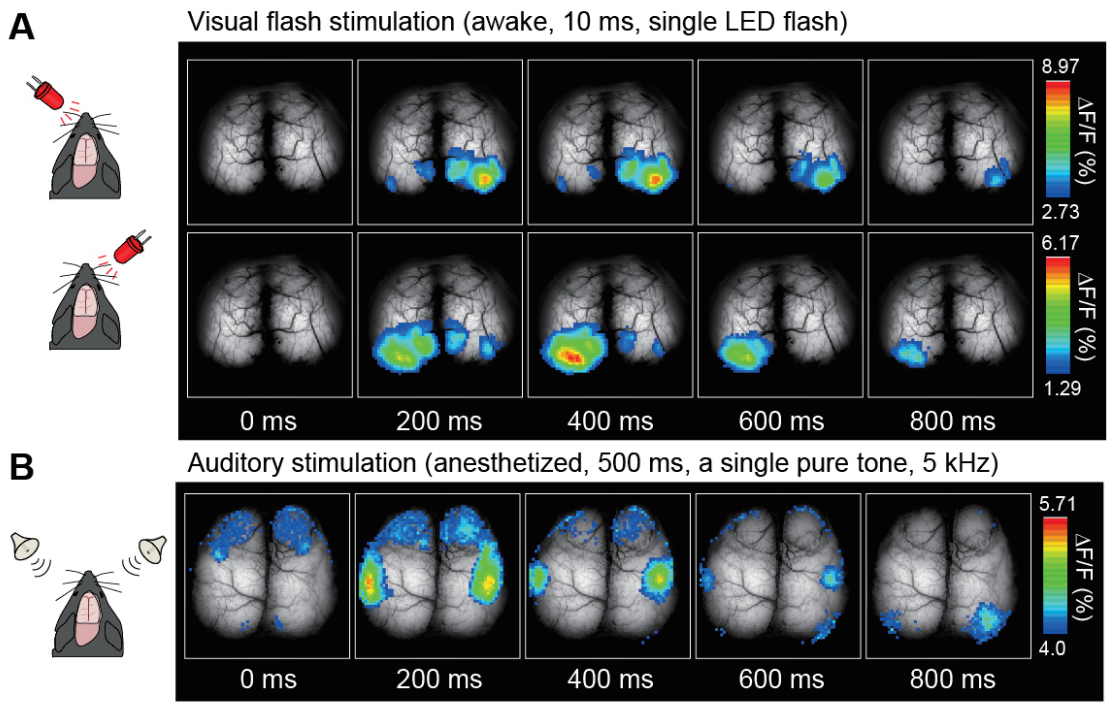

Fig. 3. Examples of cortical sensory mapping. Visual stimuli (A) and auditory stimuli (B) were applied. Pseudocolor is superimposed on the raw brain images, which represents the fluorescence change ratio. The sampling rate was 30 Hz (Modified from Monai et al., 2016 [5]).

Meanwhile, it has been reported that general anesthesia significantly reduces spontaneous astrocytic Ca^{2+} activities [42]. Moreover, as the kinetics of astrocytic Ca^{2+} dynamics are much slower than that of neurons, astrocytic Ca^{2+} contribute little to spontaneous Ca^{2+} oscillations observed above. Indeed, we observed cortical cellular activities during the spontaneous state with two-photon microscopy and found almost no Ca^{2+} elevation in astrocytes under urethane anesthesia.

4. Transcranial cortex-wide Ca^{2+} imaging during sensory stimulations

Next, we tried to identify the regions where the response occurs during specific sensory stimulation. This kind of approach has been called cortical functional mapping, and people have been attempting to draw the map with voltage-sensitive dyes [31,32,43], and the Ca^{2+} sensor in sensory [4,44] and motor areas [45,46].

We have demonstrated cortical functional mappings for the different sensory modalities such as LED flash stimulation to the eyes (Fig. 3A), pure tone to the ears (Fig. 3B), and piezo vibration to the whiskers (Fig. 4A). We also confirmed that these responses to the simple stimulus are almost neuronal, not astrocytic.

The visual stimulus was applied with a single LED flash with 10 ms duration to each eye of unanesthetized mice. As shown in Figure 3A, the response in the primary visual cortices rapidly occurred 200–400 ms after flashing; on the left hemisphere by the right eye stimulation and on the right hemisphere by the left eye stimulation. The amplitude of the fluorescence change ratio from the baseline (before stimulation) was at most 10% (ΔF/F). The response time and amplitude were not different in anesthetized mice.

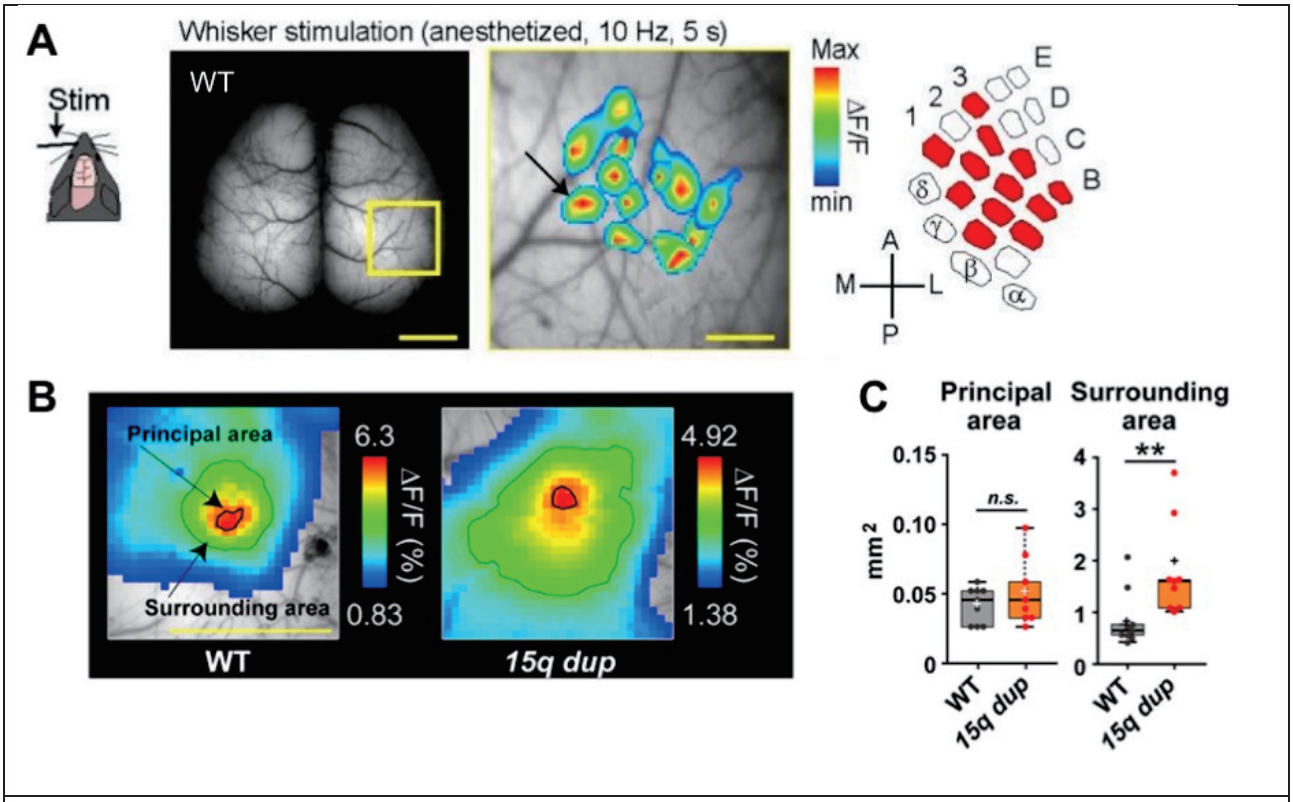

Fig. 4. Examples of cortical whisker-barrel mapping in the WT mouse and autism spectrum disorder (ASD) mouse (15q dup). (A) A single whisker was vibrated for 5 s at 10 Hz. Pseudocolor is the mean of 16 trials and superimposed 12 whisker-barrel maps on one raw image, which is magnified in the yellow square. The drawn map is similar to the classically identified whisker-barrel relationship (right). Scale bar; 1 mm (left), 250 μm (center). (B) The different whisker-evoked area distribution in WT and 15q dup mouse. The bold line around the red area represents the principal area and a thin line on the green area represents the surrounding area. (C) Comparison of areas between WT and 15q dp. Data are shown in mean ± s.e.m. **p<0.01
(Modified from Monai et al., 2016 [5] and Nakai et al., 2017 [13]).

The audible range of mice is about 1−50 kHz. Therefore, we generated 5 kHz pure tone and applied this to anesthetized mice for 500 ms. As a result, the auditory area on both hemispheres successfully responded to the sound within sub-seconds (Fig. 3B).

We next vibrated a single whisker of anesthetized mice at 10 Hz for 5 s every 60 sec with a syringe controlled by a piezoelectric device then calculated the mean of 16 trials. Figure 4A shows the graphically superimposed 12-whisker responses on the corresponding barrel cortex, which reproduced well the known whisker-barrel relationship [47,48].

5. Transcranial cortex-wide Ca^{2+} imaging with a disease model

These data were acquired from homozygous G7NG817 mice, although we found that signals in heterozygous G7NG817 mice are bright enough for transcranial imaging. Therefore, it is possible to generate various multiple transgenics, such as disease models, by just simple crossing with G7NG817, which will be useful for the first evaluation of any phenotype related to the cortical functions.

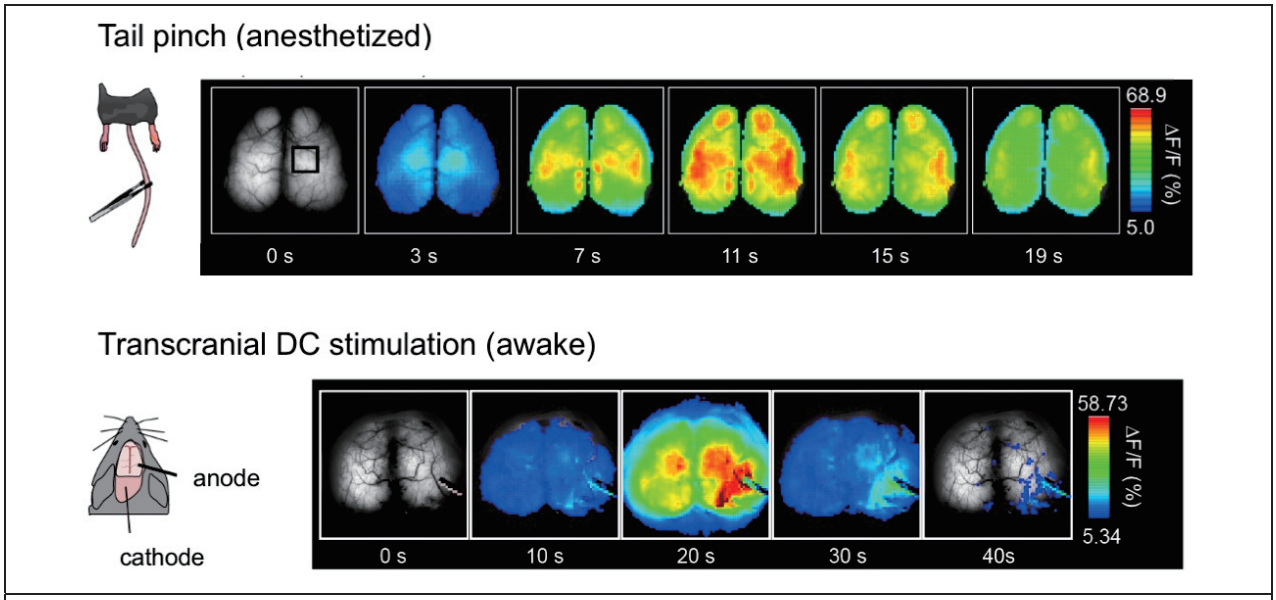

Fig. 5. Global and slow response after tail-pinch and tDCS. (top) The tail of the urethane anesthetized mouse is pinched four times for two seconds at time zero. Psudocoloring is superimposed on the raw images. (bottom) Awake mice were fixed by their head with a metal head plate attached to the skull with dental cement. tDCS anode was placed on the right hemisphere, and the cathode was on the neck muscle. Weak direct current, 0.1 mA, was applied for 10 min (Modified from Monai et al., 2016 [5]).

For example, Nakai and Takumi generated a double transgenic mouse line with G7NG817 mice and one of the autism spectrum disorder (ASD) model mice, 15q dup mice (a model for ASD with the human 15q11-13 duplication [49]) [13]. It has been shown that 15q dup mice are compromised in social communications and flexible behavior [49], with abnormal cortical spines, and cerebellar functions [50,51].

In the ASD model, the single whisker stimulation evoked area did not show any apparent changes in the "principal area." In contrast, the "surrounding area" defined by the region, which has a higher amplitude than 60% of the peak, significantly enlarged and invaded the adjacent territory (Fig. 4B-C). The principal area was defined as the region that exceeded the mean response in the 3 × 3 binned area around the peak value during 500 ms from the stimulus onset; the surrounding area was defined as the region that exceeded 60% of the mean peak amplitude during 500 ms from the stimulus onset. These observations suggest that the whisker sensory information processing in the barrel cortex could not be tuned accurately and correctly in the ASD model mice (Fig. 4B-C).

6. Transcranial cortex-wide Ca^{2+} imaging of astrocytic activities and synaptic plasticity

Urethane anesthesia induces delta waves, which show a high amplitude and synchronized slow oscillations, as known as slow-wave sleep. A sharp tail pinch stimulation induces a transition to high-frequency wave, which shows as asynchronous, low amplitude, and at about 40 Hz, as known as gamma rhythm.

We hypothesized that tail-pinch stimulation to urethane-anesthetized G7NG817 mice also could induce a global transition to high-frequency and low amplitude gamma rhythm of Ca^{2+} oscillation. However, tail-pinch caused a global response synchronized all over the cortex with ten times higher amplitude and longer duration, which is sustained for a few tens of seconds, unlike all the other sensory stimulations (Fig. 5). Cellular resolution observation using two-photon microscopy revealed that the bright and slow signals that appeared during the tail pinch were originating from astrocytes.

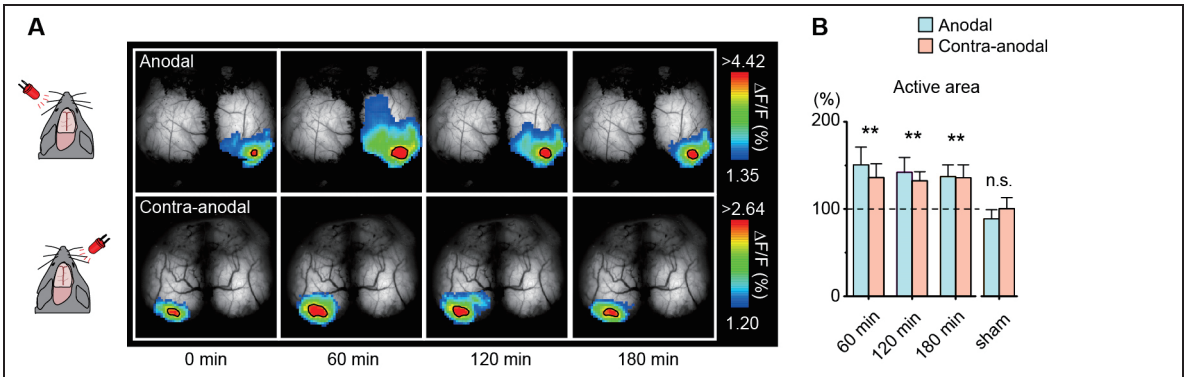

Fig. 6. (A) Transcranial imaging of visual flash response after tDCS. The flash responses to left and right-eye are plotted as anodal and contra-anodal, respectively (ipsilateral responses are masked out). The color range is between mean +1 SD and the peak value of the baseline visual evoked response. Solid black borders demarcate areas exceeding 90% of the baseline visual evoked response (active areas). (B) Comparison of the area of the visual-evoked region after tDCS. Data is mean + s.e.m. **p<0.01. (Modified from Monai et al., 2016 [5].)

The primary resource of astrocytic Ca^{2+} elevation is the intracellular release from inositol 1,4,5-trisphosphate (IP_3) receptor type 2 (IP_3R2) on the endoplasmic reticulum, which is triggered by IP_3 produced through the intracellular signaling induced by the activation of G-protein coupled receptor (GPCR) on the astrocytes' membrane. Astrocytes have various kinds of GPCR [52]. The ligands of GPCR are mainly neuromodulators, such as acetylcholine and noradrenaline. Tail pinch could induce the release of multiple neuromodulators.

We also found that the weak direct electric current stimulation on the one hemisphere through the skull induced similar Ca^{2+} response as tail pinch, that is, slowly spread all over the cortex with high amplitude (Fig. 5). This method is known as transcranial direct-current stimulation (tDCS) and has been reported that tDCS could alleviate various kinds of diseases, especially psychiatric disorders such as depression (Review in [53]). Furthermore, it has been reported that tDCS could enhance learning and memory; the underlying neural mechanisms might be a facilitation of the efficacy of the synaptic transmission, i.e., synaptic plasticity. Of note, we confirmed that tDCS-induced slow and blight Ca^{2+} response was originated from astrocytes and neurons did not show obvious change during tDCS.

To visualize the synaptic plasticity after tDCS, we repeatedly measured the LED-induced, visual-evoked area in awake mice (Fig. 6A). As a result, the area significantly enlarged within 60 min after tDCS and lasted at least 3 hours (Fig. 6B-C). We confirmed that visual-evoked potentials were also enhanced after tDCS using electrophysiological measurements.

We have reported that astrocytic IP_3/Ca^{2+} signaling plays an essential role in the mechanisms of tDCS-induced synaptic plasticity [5,40,53,54], suggesting that astrocytes are more than just supporting cells for neurons in the brain.

7. Conclusion

Transcranial cortex-wide imaging is a powerful tool to monitor brain activity continuously with a broader field of view, stable and non-invasively. Notably, the technique is useful for the initial evaluation of cortical functions in the various transgenic mouse, including the disease model. Besides, it can also visualize synaptic plasticity, which is the basis for learning and long-term memory. Moreover, standard epifluorescence microscopy is available for transcranial imaging, while it has lower resolution and more depth limitations than two-photon microscopy. Hopefully, three-photon microscopy [54,55] will soon enable us to observe deeper areas using cellular resolution without opening the skull.

References

1. N.J. Sofroniew, D. Flickinger, J. King, K. Svoboda,

A large field of view two-photon mesoscope with subcellular resolution for in vivo imaging, ELife. 5 (2016) e14472. https://doi.org/10.7554/eLife.14472.
2. C. Stringer, M. Pachitariu, N. Steinmetz, C.B. Reddy, M. Carandini, K.D. Harris, Spontaneous behaviors drive multidimensional, brainwide activity, Science. 364 (2019). https://doi.org/10.1126/science.aav7893.
3. C. Stringer, M. Pachitariu, N. Steinmetz, M. Carandini, K.D. Harris, High-dimensional geometry of population responses in visual cortex, Nature. 571 (2019) 361–365. https://doi.org/10.1038/s41586-019-1346-5.
4. M.P. Vanni, T.H. Murphy, Mesoscale Transcranial Spontaneous Activity Mapping in GCaMP3 Transgenic Mice Reveals Extensive Reciprocal Connections between Areas of Somatomotor Cortex, Journal of Neuroscience. 34 (2014) 15931–15946. https://doi.org/10.1523/JNEUROSCI.1818-14.2014.
5. H. Monai, M. Ohkura, M. Tanaka, Y. Oe, A. Konno, H. Hirai, K. Mikoshiba, S. Itohara, J. Nakai, Y. Iwai, H. Hirase, Calcium imaging reveals glial involvement in transcranial direct current stimulation-induced plasticity in mouse brain, Nature Communications. 7 (2016) 11100. https://doi.org/10.1038/ncomms11100.
6. T.H. Murphy, J.D. Boyd, F. Bolaños, M.P. Vanni, G. Silasi, D. Haupt, J.M. LeDue, High-throughput automated home-cage mesoscopic functional imaging of mouse cortex, Nature Communications. 7 (2016) 1–12. https://doi.org/10.1038/ncomms11611.
7. G. Silasi, D. Xiao, M.P. Vanni, A.C.N. Chen, T.H. Murphy, Intact skull chronic windows for mesoscopic wide-field imaging in awake mice, Journal of Neuroscience Methods. 267 (2016) 141–149. https://doi.org/10.1016/j.jneumeth.2016.04.012.
8. Y. Xie, A.W. Chan, A. McGirr, S. Xue, D. Xiao, H. Zeng, T.H. Murphy, Resolution of High-Frequency Mesoscale Intracortical Maps Using the Genetically Encoded Glutamate Sensor iGluSnFR, J. Neurosci. 36 (2016) 1261–1272. https://doi.org/10.1523/JNEUROSCI.2744-15.2016.
9. W.E. Allen, I.V. Kauvar, M.Z. Chen, E.B. Richman, S.J. Yang, K. Chan, V. Gradinaru, B.E. Deverman, L. Luo, K. Deisseroth, Global Representations of Goal-Directed Behavior in Distinct Cell Types of Mouse Neocortex, Neuron. 94 (2017) 891-907.e6. https://doi.org/10.1016/j.neuron.2017.04.017.
10. M. Balbi, M.P. Vanni, G. Silasi, Y. Sekino, L. Bolanos, J.M. LeDue, T.H. Murphy, Targeted ischemic stroke induction and mesoscopic imaging assessment of blood flow and ischemic depolarization in awake mice, NPh. 4 (2017) 035001. https://doi.org/10.1117/1.NPh.4.3.035001.
11. H. Makino, C. Ren, H. Liu, A.N. Kim, N. Kondapaneni, X. Liu, D. Kuzum, T. Komiyama, Transformation of Cortex-wide Emergent Properties during Motor Learning, Neuron. 94 (2017) 880-890.e8. https://doi.org/10.1016/j.neuron.2017.04.015.
12. A. McGirr, J. LeDue, A.W. Chan, Y. Xie, T.H. Murphy, Cortical functional hyperconnectivity in a mouse model of depression and selective network effects of ketamine, Brain. 140 (2017) 2210–2225. https://doi.org/10.1093/brain/awx142.
13. N. Nakai, M. Nagano, F. Saitow, Y. Watanabe, Y. Kawamura, A. Kawamoto, K. Tamada, H. Mizuma, H. Onoe, Y. Watanabe, H. Monai, H. Hirase, J. Nakatani, H. Inagaki, T. Kawada, T. Miyazaki, M. Watanabe, Y. Sato, S. Okabe, K. Kitamura, M. Kano, K. Hashimoto, H. Suzuki, T. Takumi, Serotonin rebalances cortical tuning and behavior linked to autism symptoms in 15q11-13 CNV mice, Science Advances. 3 (2017) e1603001. https://doi.org/10.1126/sciadv.1603001.
14. M.P. Vanni, A.W. Chan, M. Balbi, G. Silasi, T.H. Murphy, Mesoscale Mapping of Mouse Cortex Reveals Frequency-Dependent Cycling between Distinct Macroscale Functional Modules, J. Neurosci. 37 (2017) 7513–7533. https://doi.org/10.1523/JNEUROSCI.3560-16.2017.
15. A. Gilad, Y. Gallero-Salas, D. Groos, F. Helmchen, Behavioral Strategy Determines Frontal or Posterior Location of Short-Term Memory in Neocortex, Neuron. 99 (2018) 814-828.e7. https://doi.org/10.1016/j.neuron.2018.07.029.
16. S. Kuroki, T. Yoshida, H. Tsutsui, M. Iwama, R. Ando, T. Michikawa, A. Miyawaki, T. Ohshima, S. Itohara, Excitatory Neuronal Hubs Configure Multisensory Integration of Slow Waves in Association Cortex, Cell Reports. 22 (2018) 2873–2885. https://doi.org/10.1016/j.celrep.2018.02.056.
17. L. Zhu, C.R. Lee, D.J. Margolis, L. Najafizadeh, Decoding cortical brain states from widefield calcium imaging data using visibility graph, Biomed Opt Express. 9 (2018) 3017–3036. https://doi.org/10.1364/BOE.9.003017.
18. M. Balbi, M.P. Vanni, M.J. Vega, G. Silasi, Y. Sekino, J.D. Boyd, J.M. LeDue, T.H. Murphy, Longitudinal monitoring of mesoscopic cortical

activity in a mouse model of microinfarcts reveals dissociations with behavioral and motor function, J Cereb Blood Flow Metab. 39 (2019) 1486–1500. https://doi.org/10.1177/0271678X18763428.
19. L.M. Brier, E.C. Landsness, A.Z. Snyder, P.W. Wright, G.A. Baxter, A.Q. Bauer, J.-M. Lee, J.P. Culver, Separability of calcium slow waves and functional connectivity during wake, sleep, and anesthesia, NPh. 6 (2019) 035002. https://doi.org/10.1117/1.NPh.6.3.035002.
20. K.B. Clancy, I. Orsolic, T.D. Mrsic-Flogel, Locomotion-dependent remapping of distributed cortical networks, Nature Neuroscience. 22 (2019) 778–786. https://doi.org/10.1038/s41593-019-0357-8.
21. J.V. Cramer, B. Gesierich, S. Roth, M. Dichgans, M. Düring, A. Liesz, In vivo widefield calcium imaging of the mouse cortex for analysis of network connectivity in health and brain disease, NeuroImage. 199 (2019) 570–584. https://doi.org/10.1016/j.neuroimage.2019.06.014.
22. M. Li, S. Gui, Q. Huang, L. Shi, J. Lu, P. Li, Density center-based fast clustering of widefield fluorescence imaging of cortical mesoscale functional connectivity and relation to structural connectivity, Neurophotonics. 6 (2019) 045014. https://doi.org/10.1117/1.NPh.6.4.045014.
23. N.J. Michelson, M.P. Vanni, T.H. Murphy, Comparison between transgenic and AAV-PHP.eB-mediated expression of GCaMP6s using in vivo wide-field functional imaging of brain activity, Neurophotonics. 6 (2019) 025014. https://doi.org/10.1117/1.NPh.6.2.025014.
24. K. O'Hashi, K. Sohya, H. Matsuno, S. Tsuchimine, H. Kunugi, Construction of the common cortical space by spontaneous activity and its application in the mouse cortex, Biochem. Biophys. Res. Commun. 513 (2019) 869–874. https://doi.org/10.1016/j.bbrc.2019.04.048.
25. A. Gilad, F. Helmchen, Spatiotemporal refinement of signal flow through association cortex during learning, Nature Communications. 11 (2020) 1–14. https://doi.org/10.1038/s41467-020-15534-z.
26. V.A. Kalatsky, M.P. Stryker, New Paradigm for Optical Imaging: Temporally Encoded Maps of Intrinsic Signal, Neuron. 38 (2003) 529–545. https://doi.org/10.1016/S0896-6273(03)00286-1.
27. A. Zepeda, C. Arias, F. Sengpiel, Optical imaging of intrinsic signals: recent developments in the methodology and its applications, Journal of Neuroscience Methods. 136 (2004) 1–21. https://doi.org/10.1016/j.jneumeth.2004.02.025.
28. S. Schuett, T. Bonhoeffer, M. Hübener, Mapping Retinotopic Structure in Mouse Visual Cortex with Optical Imaging, J. Neurosci. 22 (2002) 6549–6559. https://doi.org/10.1523/JNEUROSCI.22-15-06549.2002.
29. M. Tohmi, K. Takahashi, Y. Kubota, R. Hishida, K. Shibuki, Transcranial flavoprotein fluorescence imaging of mouse cortical activity and plasticity, Journal of Neurochemistry. 109 (2009) 3–9. https://doi.org/10.1111/j.1471-4159.2009.05926.x.
30. K. Takahashi, R. Hishida, Y. Kubota, M. Kudoh, S. Takahashi, K. Shibuki, Transcranial fluorescence imaging of auditory cortical plasticity regulated by acoustic environments in mice, European Journal of Neuroscience. 23 (2006) 1365–1376. https://doi.org/10.1111/j.1460-9568.2006.04662.x.
31. I. Ferezou, F. Haiss, L.J. Gentet, R. Aronoff, B. Weber, C.C.H. Petersen, Spatiotemporal Dynamics of Cortical Sensorimotor Integration in Behaving Mice, Neuron. 56 (2007) 907–923. https://doi.org/10.1016/j.neuron.2007.10.007.
32. M.H. Mohajerani, A.W. Chan, M. Mohsenvand, J. LeDue, R. Liu, D.A. McVea, J.D. Boyd, Y.T. Wang, M. Reimers, T.H. Murphy, Spontaneous cortical activity alternates between motifs defined by regional axonal projections, Nature Neuroscience. 16 (2013) 1426–1435. https://doi.org/10.1038/nn.3499.
33. A. Stroh, H. Adelsberger, A. Groh, C. Rühlmann, S. Fischer, A. Schierloh, K. Deisseroth, A. Konnerth, Making Waves: Initiation and Propagation of Corticothalamic Ca2+ Waves In Vivo, Neuron. 77 (2013) 1136–1150. https://doi.org/10.1016/j.neuron.2013.01.031.
34. T. Matsui, T. Murakami, K. Ohki, Transient neuronal coactivations embedded in globally propagating waves underlie resting-state functional connectivity, PNAS. 113 (2016) 6556–6561. https://doi.org/10.1073/pnas.1521299113.
35. Y. Ma, M.A. Shaik, S.H. Kim, M.G. Kozberg, D.N. Thibodeaux, H.T. Zhao, H. Yu, E.M.C. Hillman, Wide-field optical mapping of neural activity and brain haemodynamics: considerations and novel approaches, Philosophical Transactions of the Royal Society B: Biological Sciences. 371 (2016) 20150360. https://doi.org/10.1098/rstb.2015.0360.
36. T.-W. Chen, N. Li, K. Daie, K. Svoboda, A Map of Anticipatory Activity in Mouse Motor Cortex, Neuron. 94 (2017) 866-879.e4. https://doi.org/10.1016/j.neuron.2017.05.005.
37. L.F. Rossi, R.C. Wykes, D.M. Kullmann, M. Carandini, Focal cortical seizures start as standing waves and propagate respecting homotopic connectivity, Nature Communications. 8 (2017) 1–11.

https://doi.org/10.1038/s41467-017-00159-6.
38. M. Carandini, D. Shimaoka, L.F. Rossi, T.K. Sato, A. Benucci, T. Knöpfel, Imaging the Awake Visual Cortex with a Genetically Encoded Voltage Indicator, J. Neurosci. 35 (2015) 53–63. https://doi.org/10.1523/JNEUROSCI.0594-14.2015.
39. M. Ohkura, T. Sasaki, J. Sadakari, K. Gengyo-Ando, Y. Kagawa-Nagamura, C. Kobayashi, Y. Ikegaya, J. Nakai, Genetically encoded green fluorescent Ca2+ indicators with improved detectability for neuronal Ca2+ signals., PloS One. 7 (2012) e51286. https://doi.org/10.1371/journal.pone.0051286.
40. T. Mishima, T. Nagai, K. Yahagi, S. Akther, Y. Oe, H. Monai, S. Kohsaka, H. Hirase, Transcranial Direct Current Stimulation (tDCS) Induces Adrenergic Receptor-Dependent Microglial Morphological Changes in Mice, ENeuro. 6 (2019). https://doi.org/10.1523/ENEURO.0204-19.2019.
41. L. de Vivo, M. Melone, J.D. Rothstein, F. Conti, GLT-1 Promoter Activity in Astrocytes and Neurons of Mouse Hippocampus and Somatic Sensory Cortex., Frontiers in Neuroanatomy. 3 (2010) 31. https://doi.org/10.3389/neuro.05.031.2009.
42. A.S. Thrane, V.R. Thrane, D. Zeppenfeld, N. Lou, Q. Xu, E.A. Nagelhus, M. Nedergaard, V. Rangroo Thrane, General anesthesia selectively disrupts astrocyte calcium signaling in the awake mouse cortex, Proc Natl Acad Sci U S A. 109 (2012) 18974–18979. https://doi.org/1209448109 [pii] 10.1073/pnas.1209448109.
43. D.H. Lim, M.H. Mohajerani, J. LeDue, J. Boyd, S. Chen, T.H. Murphy, In vivo Large-Scale Cortical Mapping Using Channelrhodopsin-2 Stimulation in Transgenic Mice Reveals Asymmetric and Reciprocal Relationships between Cortical Areas, Front. Neural Circuits. 6 (2012). https://doi.org/10.3389/fncir.2012.00011.
44. I.R. Winship, T.H. Murphy, In Vivo Calcium Imaging Reveals Functional Rewiring of Single Somatosensory Neurons after Stroke, J. Neurosci. 28 (2008) 6592–6606. https://doi.org/10.1523/JNEUROSCI.0622-08.2008.
45. O.G.S. Ayling, T.C. Harrison, J.D. Boyd, A. Goroshkov, T.H. Murphy, Automated light-based mapping of motor cortex by photoactivation of channelrhodopsin-2 transgenic mice, Nature Methods. 6 (2009) 219–224. https://doi.org/10.1038/nmeth.1303.
46. R. Hira, N. Honkura, J. Noguchi, Y. Maruyama, G.J. Augustine, H. Kasai, M. Matsuzaki, Transcranial optogenetic stimulation for functional mapping of the motor cortex, Journal of Neuroscience Methods. 179 (2009) 258–263. https://doi.org/10.1016/j.jneumeth.2009.02.001.
47. K.L. Bernardo, J.S. McCasland, T.A. Woolsey, R.N. Strominger, Local intra- and interlaminar connections in mouse barrel cortex, Journal of Comparative Neurology. 291 (1990) 231–255. https://doi.org/10.1002/cne.902910207.
48. D.J. Margolis, H. Lütcke, K. Schulz, F. Haiss, B. Weber, S. Kügler, M.T. Hasan, F. Helmchen, Reorganization of cortical population activity imaged throughout long-term sensory deprivation, Nature Neuroscience. 15 (2012) 1539–1546. https://doi.org/10.1038/nn.3240.
49. J. Nakatani, K. Tamada, F. Hatanaka, S. Ise, H. Ohta, K. Inoue, S. Tomonaga, Y. Watanabe, Y.J. Chung, R. Banerjee, K. Iwamoto, T. Kato, M. Okazawa, K. Yamauchi, K. Tanda, K. Takao, T. Miyakawa, A. Bradley, T. Takumi, Abnormal Behavior in a Chromosome- Engineered Mouse Model for Human 15q11-13 Duplication Seen in Autism, Cell. 137 (2009) 1235–1246. https://doi.org/10.1016/j.cell.2009.04.024.
50. M. Isshiki, S. Tanaka, T. Kuriu, K. Tabuchi, T. Takumi, S. Okabe, Enhanced synapse remodelling as a common phenotype in mouse models of autism, Nat Commun. 5 (2014) 4742. https://doi.org/10.1038/ncomms5742.
51. C. Piochon, A.D. Kloth, G. Grasselli, H.K. Titley, H. Nakayama, K. Hashimoto, V. Wan, D.H. Simmons, T. Eissa, J. Nakatani, A. Cherskov, T. Miyazaki, M. Watanabe, T. Takumi, M. Kano, S.S.-H. Wang, C. Hansel, Cerebellar plasticity and motor learning deficits in a copy-number variation mouse model of autism, Nature Communications. 5 (2014) 1–13. https://doi.org/10.1038/ncomms6586.
52. J.T. Porter, K.D. McCarthy, Astrocytic neurotransmitter receptors in situ and in vivo, Prog Neurobiol. 51 (1997) 439–455.
53. H. Monai, H. Hirase, Astrocytes as a target of transcranial direct current stimulation (tDCS) to treat depression, Neuroscience Research. 126 (2018) 15–21. https://doi.org/10.1016/j.neures.2017.08.012.

Acknowledgment

This work was supported by KAKENHI grants (18K14859, 20K15895) and the TERUMO life science foundation. The author thanks Dr. Hajime Hirase for the supervise. The author also thanks members of the laboratory for their support. The author declares no competing financial interests